Molecular Dynamics Simulations of Poly(ethylene oxide)/LiI Melts. 2. Dynamic Properties

Oleg Borodin and Grant D. Smith*

Department of Chemical and Fuels Engineering and Department of Materials Science and Engineering, University of Utah, 122 S. Central Campus Drive Rm. 304, Salt Lake City, Utah 84112

Received August 23, 1999; Revised Manuscript Received January 10, 2000

ABSTRACT: Molecular dynamics simulations have been performed on solutions of low molecular weight poly(ethylene oxide) (PEO) and LiI at 363 and 450 K for compositions ether oxygen:Li (EO:Li) = 48:1, 15:1, and 5:1. An explicit atom quantum chemistry based force field has allowed us to make quantitative predictions of polymer dynamics, ion mobilities, and complex lifetimes in these solutions. In the more dilute PEO/LiI solutions we found dynamical behavior consistent with a separation of the solutions into salt-rich and polymer-rich (PEO-like) domains. Dihedrals with oxygen atoms bound to Li^+ cations (complexed dihedrals) were found to have significantly slower conformational dynamics than those dihedrals not bound to Li^+ cations (uncomplexed dihedrals). In the dilute solutions, the dynamics of the complexed dihedrals were found to be only weakly dependent on composition, and the dynamics of the uncomplexed dihedrals were found to resemble closely those of pure PEO. For the EO:Li = 5:1 system, the conformational dynamics of both complexed and uncomplexed dihedrals were dramatically slower than in the more dilute solutions, and it was no longer possible to observe dynamical behavior consistent with separate salt-rich and polymer-rich domains. A slowing down of polymer chain dynamics with increasing salt concentration, characterized by a significant increase in the Rouse time and a significant decrease in the polymer self-diffusion coefficient, was also observed. Chain dynamics exhibited behavior consistent with salt-rich and PEO-rich domains for EO:Li ≥ 15:1. The slowing down of chain dynamics was found to be correlated with an increase in the torsional correlation time due to restriction of the conformational space available for complexed dihedrals, resembling behavior seen in simulations of polymer melts approaching the glass-transition temperature. The ether oxygen−cation bond was found to be quite labile, with an average lifetime of approximately 100−200 ps, while cations translate the length of a polymer chain on a nanosecond time scale. Despite the high lability of the ether oxygen−cation bonds, interchain hopping events were rare, with an estimated frequency of 1 interchain hop/cation/10−100 ns. For systems with Rouse times less than the hopping time, we found the ion mobilities to be highly correlated with the polymer center-of-mass motion. For the EO:Li = 5:1 solutions with much longer Rouse times and a lightly cross-linked system, some decoupling of the ion motion from polymer motion, indicative of a change in mechanism, was observed. Finally, in contrast to previous simulations, conductivities and ion self-diffusion coefficients were predicted to within 1 order of magnitude of experimental values for similar systems.

I. Introduction

Polymer electrolytes are of interest for use in secondary batteries, variable transmission windows, and displays. They combine ease of fabrication, low flammability, and toxicity with the ability to form good interfacial contact with electrodes.[1,2] Poly(ethylene oxide) (PEO) is one of the most widely studied polymer hosts for polymer electrolytes. There is also increasing interest in the use of low molecular weight PEO as a nonvolatile plasticizer in host polymers such as poly(vinylidene fluoride),[3] cross-linked PEO,[4] and photopolymerized oligo(ethylene glycol)$_{23}$ with dimethyl acrylate.[5] Hence, a better understanding of the structure and dynamics of PEO−salt complexes could play a key role in the development of improved polymer electrolytes.

Molecular dynamics (MD) simulations can be a powerful tool for obtaining new insight into polymer electrolytes by providing atomistic detail of both structure and dynamics. The primary limitations in applying MD simulation techniques to the study of polymer electrolytes are the accessible time scales and the accuracy of the potential energy functions used to describe intramolecular and intermolecular interactions. Experimental studies of the molecular weight dependence of the conductivity of polymer electrolytes[6] and theoretical treatments[6,7] indicate that, for polymer/alkali salt systems with polymer host chains below the entanglement molecular weight, the Rouse time is the relevant time scale in determining conductivity. Hence, it is highly desirable to perform MD simulations on polymer electrolytes with trajectories comparable to the Rouse time (τ_R) of the simulated systems. While previous MD simulations of PEO/LiI[8,9] and PEO/NaI[10] melts have provided insight into the dynamics of these systems, the short trajectories ($\ll\tau_R$) and qualitative nature of the potentials employed precluded the authors from making quantitative predictions of dynamic properties of the systems, including conductivities. In our study, much longer trajectories have been generated, and the PEO chain length and simulation temperatures were chosen so as to make the relevant time scales accessible.

In our previous paper[11] we examined the structural and conformational properties of PEO/LiI solutions as a function of salt concentration and temperature. These simulations were performed at temperatures above the melting point of PEO using relatively low molecular weight PEO chains (12 repeat units, M_w = 540 Da). The simulations were performed using a quantum chemistry based potential[12,13] that has been demonstrated to accurately reproduce the energetics of Li^+−ether interactions, the solvation environment of Li^+ cations,[14] and the conformations[15] and dynamics[16] of the pure PEO

10.1021/ma991429h CCC: $19.00
Published on Web 03/01/2000

melts. In this paper, we examine in detail the dynamics of the PEO/LiI solutions as a function of salt concentration and temperature. Because ion conductivity in polymer electrolytes occurs in the amorphous phase,[17] MD simulations performed at temperatures above the melting point of the polymer, such as those reported here, can provide valuable insight into the conformational and dynamic properties of PEO−salt systems relevant to their room-temperature application.

In section II we briefly describe the potential functions and simulation methodology employed. In section III we investigate the influence of salt on polymer conformational dynamics and polymer chain dynamics. The latter are accessible from our simulations because of our use of ensembles of low molecular weight chains. In section IV we investigate the dynamics of oxygen−cation bonding and cation−anion bonding. Section V explores ion mobilities and the conductivity of the solutions. The ability of our simulations to reproduce available experimental data on related systems is evaluated. Finally, in section VI the influence of salt on polymer dynamics and the relationship between polymer dynamics and ion mobilities are summarized and discussed.

II. Force Field and Simulation Methodology

Molecular dynamics simulations were performed on PEO/LiI melts composed of 32 PEO chains of 12 repeat units with a structure H−[CH_2OCH_2]$_{12}$−H. Simulations were performed for the pure PEO melt as well as the systems having the following ether oxygen:Li (EO:Li) ratios; EO:Li = 48:1, EO:Li = 15:1, and EO:Li = 5:1 (ratios were rounded). Simulations were performed at 363 and 450 K. A quantum chemistry based potential function described elsewhere[12−13,18] was used. The bond lengths were constrained using the Shake algorithm.[19] For most of the systems studied, the simulation trajectories were 5 ns or longer. The simulation methodology, including equilibration procedure, is described in detail in a previous paper.[11] The static properties of the solutions as a function of salt concentration and temperature have been previously published.[11]

III. Polymer Dynamics

It is known that addition of salt results in a slowing down of polymer dynamics. For example, it has been observed that the onset of the glass transition in PEO and PPO based polymer electrolytes occurs at higher temperature with increasing salt content.[20,21] The slowing down of polymer dynamics leads to a reduction in ion mobilities and hence reduced molar conductivity with increasing salt concentration.[1,22] It is therefore important to understand both the influence of salt on polymer dynamics and the relationship between polymer dynamics and ion mobilities. While it is clear that salt slows the polymer, the mechanism is uncertain. In this section we examine the influence of salt on both polymer conformational dynamics and polymer chain dynamics.

A. Conformational Dynamics. 1. Overall Conformational Dynamics. The average conformational transition time $\langle\tau_{\text{transition}}\rangle$, defined as the total trajectory time divided by the average number of transitions per dihedral, is a fundamental time scale in the consideration of polymer dynamics. The conformational transition times for the PEO/LiI solutions as a function of salt concentration and temperature are tabulated in Table 1. While $\langle\tau_{\text{transition}}\rangle$ increases with increasing salt concentration as well as with decreasing temperature, the influence of salt on the average conformational transition time is not dramatic.

Table 1. Average Conformational Transition Time $\langle\tau_{\text{transition}}\rangle$ (ps)

	−C−O− dihedrals		−C−C− dihedrals	
system	450 K	363 K	450 K	363 K
pure PEO	4.2	7.1	4.9	8.4
48:1	4.6	7.6	5.2	9.0
15:1	5.2	9.8	6.4	13.3
5:1	7.6	13.4	11.5	21.1

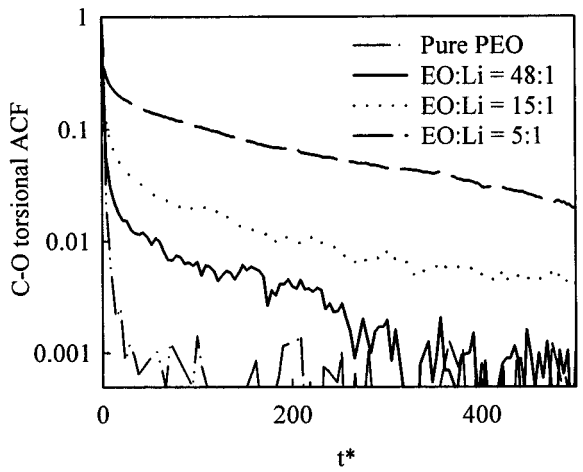

Figure 1. Torsional autocorrelation function for C−O dihedrals at 450 K. Time (t^*) is given in reduced units (average number of conformational transitions).

Conformational dynamics can also be investigated by monitoring the torsional autocorrelation functions (TACF). Let $H_i(t)$ be the characteristic function of the dihedral state $i = \{t,g^+,g^-\}$ at time t. $H_i(t) = 1$ if the dihedral is in state i at time t, and $H_i(t) = 0$ otherwise. Three autocorrelation ($i = j$) and three cross-correlation ($i \neq j$) functions can be defined for each dihedral type in the following way:[8]

$$P_{ij}(t) = \frac{\langle (H_i(0) - \langle H_i\rangle)(H_j(t) - \langle H_j\rangle)\rangle}{\langle (H_i(0) - \langle H_i\rangle)(H_j(0) - \langle H_j\rangle)\rangle} \qquad (1)$$

where $\langle\ \rangle$ denotes an ensemble average over all dihedrals of this type. For the autocorrelation functions, eq 1 reduces to

$$P_{ii}(t) = \frac{\langle H_i(0)\, H_i(t)\rangle - \langle H_i\rangle^2}{\langle H_i^2\rangle - \langle H_i\rangle^2} \qquad (2)$$

for equilibrated systems. After sufficiently long times, $H_i(0)$ and $H_i(t)$ are completely uncorrelated; hence, $\langle H_i(0)\, H_i(t)\rangle = \langle H_i\rangle^2$ and the TACF decays to zero. We also define an average TACF for each dihedral type (−C−C− or −C−O−) $P_{\text{av}}(t)$,

$$P_{\text{av}}(t) = s_t P_{tt}(t) + s_{g+} P_{g+g+}(t) + s_{g-} P_{g-g-}(t) \qquad (3)$$

where s_i is the probability for the dihedral to be in the state $i = \{t,g^+,g^-\}$ and $P_{ii}(t)$ is the above-defined TACF.

The TACF (eq 3) as a function of t^* for −C−O− dihedrals is shown in Figure 1 for each composition at 450 K. Here, t^* is reduced time defined as the total time divided by the average conformational transition time

for a given system (Table 1) and hence is equal to the average number of transitions per dihedral. The TACF for the −C−C− dihedrals (not shown) exhibit similar behavior. Figure 1 reveals that, even on a reduced time scale, the TACF decays more slowly with increasing salt concentration. While most of the decay of the TACF occurs after only a few transitions, an increasingly large fraction of the decay occurs over much longer time scales within increasing salt concentration.

Comparing the TACF (Figure 1) and the conformational transition times (Table 1) for PEO, it can be seen that the influence of salt is much greater on the TACF than on the rate of conformational transitions. Similar behavior is seen for pure PEO[16] and polyethylene melts[25] with decreasing temperature. To resolve the apparent incongruity between the influence of salt on the conformational transition time and the TACF, we need to consider how the TACF decays. At short times, all transitions for a given dihedral will contribute to the decorrelation of $H_i(0)$ and $H_i(t)$ and hence the decay of the TACF. However, in order for the TACF to completely decay, each dihedral must explore all of conformational space (i.e., each conformational state) with equilibrium probability. Restrictions on the conformational space available for dihedrals that result in repeated jumps between two states, e.g., g^+ and t, and that exclude the third state do not strongly influence the total number of transitions and hence the conformational transition time. However, such restricted transitions are ineffective (after the initial decay) in decorrelating the conformational states as required for complete decay of the TACF. Such nonergodic behavior has been observed in pure polymer melts with decreasing temperature[16,25] and is observed in our simulations of PEO/LiI with increasing salt concentration, accounting for the greater influence of salt on the TACF compared to the conformational transition time.

2. Heterogeneity in Conformational Dynamics. It is of interest to determine whether the influence of salt on the conformational transition times in PEO (Table 1) is homogeneous (effects all dihedrals equally) or heterogeneous. We analyzed the number of conformational transitions for each dihedral after a long trajectory for each system. Results for the EO:Li = 48:1 system at 363 K over a 5.6 ns trajectory are shown in Figure 2. Figure 2 indicates that while a majority of the −C−C− dihedrals have undergone a similar number of conformational transitions after 5.6 ns, or $t^* = 622$, there are many dihedrals that have experienced from 2 to 5 times fewer conformational transitions than average. These results are consistent with the interaction model previously proposed for PPO−LiX electrolytes.[23,24]

The dynamically heterogeneous behavior seen in the rate of conformational transitions motivated us to look for other heterogeneities. The total complexation time (the time a given dihedral spends complexed during the trajectory) for the EO:Li = 48:1 system at 363 K is shown in Figure 2 for a 5.6 ns trajectory. A dihedral is considered complexed when any Li^+ cation is found in the first coordination shell of one of its ether oxygen atoms, i.e., within 4.0 Å from an ether oxygen atom belonging to the dihedral (O−C−C−O or C−O−C−C). We found that, as with the number of transitions, the total complexation time of the dihedrals varies greatly, even after times comparable to the Rouse time (5.4 ns for this system, see below).

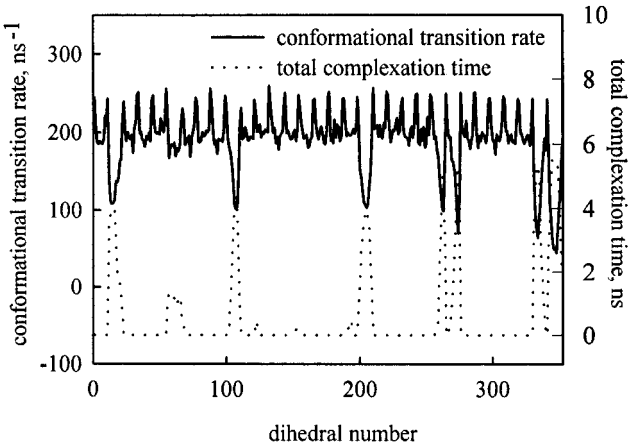

Figure 2. Correlation between the conformational transition rate (solid line) and the total complexation time (dotted line) over the simulation run (5.6 ns) for each C−C dihedral. Results for the PEO/LiI system at 363 K and EO:Li = 48:1 are presented. Noticeable periodicity in the conformational transition rate is due to a higher number of conformational transitions of the C−C dihedrals near chain ends.

3. Dynamics of Complexed and Uncomplexed Dihedrals. It is clear from Figure 2 that there is a strong correlation between the conformational transition rate of a dihedral and its complexation with Li^+ cations. As cations often stay near a particular ether oxygen atom for hundreds of picoseconds or longer (see for example Figure 2), it is possible to calculate TACF (eq 3) for complexed and uncomplexed dihedrals individually. We found that the decay of the TACF from 1 to 0.1 for both complexed and uncomplexed −C−O− and −C−C− dihedrals could be adequately characterized by the Kohlrausch−Williams−Watts (KWW) expression:

$$P_{\mathrm{KWW}}(t) = \exp[-(t/\tau)^{\beta}] \qquad (4)$$

Parameters of the KWW fits for the complexed and uncomplexed dihedrals, as well as the fraction of each, are given in Table 2. (Note that longer-time behavior of the TACF cannot be well described by a KWW function.) Comparison of the KWW parameters allows us to examine quantitatively the influence of salt concentration and temperature on the conformational dynamics of complexed and uncomplexed dihedrals, as well as to compare the conformational dynamics of uncomplexed dihedrals with those in pure PEO.

The principal relaxation time τ is much longer for complexed dihedrals compared to that for uncomplexed dihedrals for all salt concentrations. The values of τ and β for both complexed and uncomplexed dihedrals exhibit only weak dependence on salt concentration for EO:Li ≥ 15:1, particularly at 450 K. For this concentration range, the conformational dynamics of the uncomplexed dihedrals closely resemble those of pure PEO. For EO:Li = 5:1, the dynamics of the uncomplexed and complexed dihedrals differ significantly from those found at lower salt concentrations; the principal relaxation times are longer, and the processes are broader. As expected, the principal relaxation time increases with decreasing temperature in all cases.

Division of the dihedrals into fast uncomplexed dihedrals and slow complexed dihedrals whose properties (but not proportion) are independent of composition for EO:Li ≥ 15:1 is clearly reasonable. This is consistent with our previous structural analysis of these systems

Table 2. KWW Parameters for TACF for Uncomplexed and Complexed Dihedrals

		uncomplexed dihedrals						complexed dihedrals					
		450 K			363 K			450 K			363 K		
system	dihedral	fraction	τ (ps)	β	fraction	τ (ps)	β	fraction	τ (ps)	β	fraction	τ (ps)	β
pure melt	−C−O−	1.00	1.8	0.63	1.00	4.7	0.57	0.00			0.00		
48:1	−C−O−	0.90	2.1	0.61	0.90	5.4	0.46	0.10	24	0.37	0.10	178	0.36
15:1	−C−O−	0.68	1.9	0.59	0.58	8.3	0.37	0.32	26	0.37	0.42	406	0.34
5:1	−C−O−	0.19	2.8	0.38	0.15	82	0.16	0.81	69	0.25	0.85	2700	0.22
pure melt	−C−C−	1.00	5.2	0.55	1.00	19	0.52	0.00			0.00		
48:1	−C−C−	0.89	5.8	0.54	0.89	24	0.49	0.11	22	0.53	0.11	174	0.57
15:1	−C−C−	0.66	6.4	0.52	0.56	53	0.47	0.34	28	0.55	0.44	189	0.52
5:1	−C−C−	0.17	13	0.40	0.12	165	0.27	0.83	55	0.41	0.88	643	0.38

Table 3. Conformational Transition Rates (ns^{-1}) for Uncomplexed and Complexed Dihedrals

		uncomplexed dihedrals				complexed dihedrals			
		$t \leftrightarrow g^{\mp}$		$g^{\pm} \leftrightarrow g^{\mp}$		$t \leftrightarrow g^{\pm}$		$g^{\pm} \leftrightarrow g^{\mp}$	
system	dihedral	450 K	363 K	450 K	363 K	450 K	363 K	450 K	363 K
pure PEO	−C−O−	58	35	2.8	0.69				
48:1	−C−O−	56	34	2.7	0.67	25	12	0.27	0.07
15:1	−C−O−	56	31	2.6	0.54	25	14	0.21	0.04
5:1	−C−O−	48	27	1.8	0.37	24	15	0.22	0.04
pure PEO	−C−C−	50	29	2.8	0.62				
48:1	−C−C−	50	29	3.0	0.59	12	7.3	15	3.6
15:1	−C−C−	48	25	2.7	0.56	12	6.6	12	5.3
5:1	−C−C−	42	27	2.1	0.38	9.6	6.2	13	5.6

where we found that for EO:Li ≥ 15:1 the solutions can be considered as a composite of salt-rich regimes and pure PEO-like domains. Structurally, the pure PEO-like domains at EO:Li = 5:1 are much smaller than those found at lower concentrations, and this division is no longer valid. The same is seen dynamically for the high-salt content system. The EO:Li = 5:1 solutions are saturated in the sense that the dynamics of both complexed and uncomplexed dihedrals are strongly influenced by the fact that the majority of neighboring dihedrals are complexed. As shown in Table 2, approximately 80% of the dihedrals are complexed at this composition. It is worth noting that the dramatic decrease in the β parameter at EO:Li = 5:1, indicative of increased conformational cooperativity, is consistent with the behavior seen in simulations of pure polymers with decreasing temperature[25] as the glass transition is approached.

Further investigation of the conformational dynamics of complexed and uncomplexed dihedrals was carried out by monitoring their conformational transition rates, shown in Table 3. While the dynamics of dihedrals upon complexation with Li^+ cations are, in most cases, slowed by an order of magnitude or more from the point of view of the TACF (Table 2), the rate of conformational transitions is reduced only by a factor of 3 or less in most cases and, in some cases, actually increases. In addition, unlike the TACF, the conformational transition rates for the complexed dihedrals in the EO:Li = 5:1 solutions do not differ significantly from those for the lower salt content systems. This behavior is congruent with the influence of salt on the overall conformational transition rates and TACF discussed above and indicates that the primary effect of salt on polymer conformational dynamics is to restrict conformational space for complexed dihedrals, as opposed to reducing the rate of conformational transitions.

It is also worth noting that salt has a much greater effect on the rate of $g^{\pm} \leftrightarrow g^{\mp}$ transitions than on $t \leftrightarrow g^{\pm}$ transitions, as can be seen in Table 3. The rate of $g^{\pm} \leftrightarrow g^{\mp}$ transitions increases dramatically upon complexation for −C−C− dihedrals and decreases upon complexation for −C−O− dihedrals. In Figure 3, the relative free energy, $\Delta A(\phi)$, of complexed and uncomplexed −C−C− and −C−O− dihedrals is shown for the EO:Li = 15:1 at 450 K. Here,

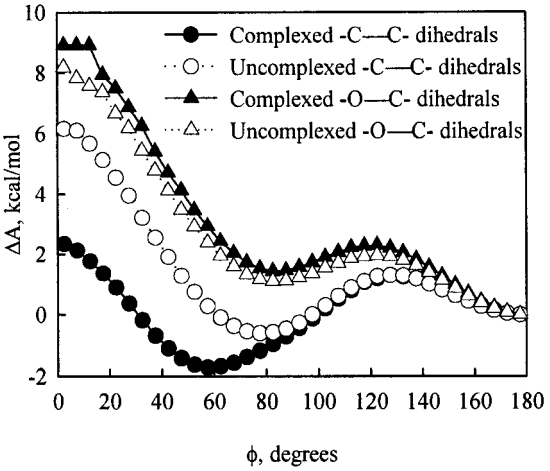

Figure 3. Helmholtz free energy as a function torsional angle relative to the trans state for complexed and uncomplexed C−C and C−O dihedrals for salt concentration EO:Li = 15:1 at 450 K.

$$\Delta A(\phi) = A(\phi) - A_{\text{trans}} = k_B T \ln \frac{p(180)}{p(\phi)} \qquad (5)$$

where $p(\phi)$ is the probability of finding the complexed or uncomplexed −C−C− or −C−O− dihedral with torsional angle ϕ, k_B is the Boltzmann constant, and T is temperature. The strong interaction of Li^+ cations with ether oxygen atoms effectively reduces the cis barrier and the energy of the gauche state relative to the trans state for the complexed −C−C− dihedrals and hence results in a dramatic increase in the rate of $g^{\pm} \leftrightarrow g^{\mp}$ transitions. Unlike the strong effect of Li^+ complexation of −C−C− dihedrals, relative free energies for C−O dihedrals change little upon complexation, resulting in approximately the same ratio of $g^{\pm} \leftrightarrow g^{\mp}$ conforma-

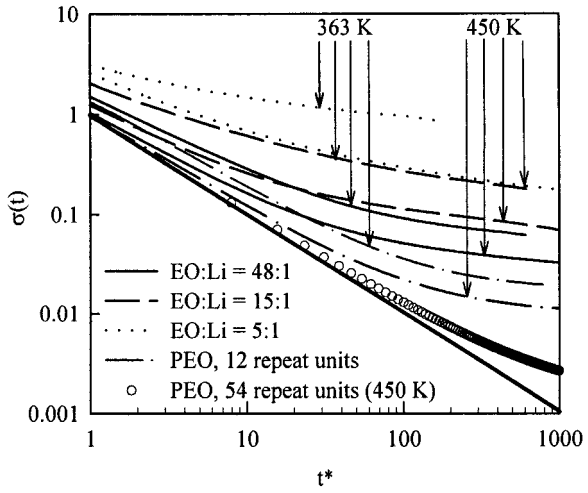

Figure 4. Width of the torsional transition rate spectrum for C—O dihedrals. Time (t^*) is given in reduced units (average number of conformational transitions). The solid line with a slope of −1 represents Poisson behavior.

tional transitions to $t \leftrightarrow g^{\pm}$ transitions for complexed and uncomplexed dihedrals.

4. Distribution of Conformational Transition Rates. We see that addition of salt not only results in an increase in the conformational transition time (Table 1) but also effects heterogeneity in the transition rates (Figure 2). The latter can be investigated quantitatively by comparing the width of the distribution of conformational transition rates $\sigma(t)$ for a particular dihedral type, defined as

$$\sigma(t) = \frac{\langle (n_i(t) - \langle n_i(t) \rangle)^2 \rangle}{\langle n_i(t) \rangle^2} \tag{6}$$

where $n_i(t)$ is the number of conformational transitions of the dihedral i after time t and $\langle\ \rangle$ denotes an average over all dihedrals of the same type, as a function of composition and temperature. Figure 4 shows $\sigma(t)$ for −C—O− dihedrals for the various compositions and temperatures investigated.

If a system exhibits homogeneous conformational dynamics, meaning that the probability that a given dihedral will be the next to undergo a transition is the same as that for all other dihedrals, conformational transitions will follow Poisson statistics. In this case, $\sigma(t) = 1/\langle n(t) \rangle = 1/t^*$, and $\sigma(t)$ approaches zero at long time. The results for a simulation of a pure melt of 54 repeat unit PEO chains at 450 K closely resemble Poisson statistics, as shown in Figure 4, for times up to $t^* = 100$. For the pure melt of 12 repeat unit PEO chains at 450 K, greater deviation from Poisson statistics is seen, indicating a more dynamically heterogeneous system. This heterogeneity is due to the increased importance of chain end effects for the shorter chains: dihedrals near the chain ends undergo transitions more rapidly than those in the chain center, and consequently $\sigma(t)$ decays to a nonzero value at long time. However, the initial slope for the pure 12 repeat unit melt at 450 K is close to unity, indicating Poisson-type behavior. Hence, we consider the pure melt of 12 repeat unit PEO at 450 K as a baseline in examining the influence of salt and temperature on conformational dynamics.

Figures 4 shows increased deviation from Poisson statistics with increasing salt concentration. Similar behavior is seen for the pure melt with decreasing temperature.[33] The long-time tail in the width of the distribution of conformational transition rates (compared to the pure 12 repeat unit melt at 450 K) indicates that some dihedrals have much slower conformational dynamics than the average dihedral on the time scale of 1000 conformational transitions. Hence, $\sigma(t)$ serves as a time-dependent measure of the heterogeneity of conformational dynamics in the system illustrated qualitatively in Figure 2 for a single system at a single time. A concentration/temperature correspondence can be seen in Figure 4. For example, the EO:Li = 5:1 system at 450 K exhibits similar behavior in its conformational dynamics to the EO:Li = 15:1 system at 363 K (see also Table 1). Concentration/temperature correspondence in the PEO/LiI solutions is further explored in section VI.

B. Polymer Chain Dynamics. Above we considered the influence of salt on polymer conformational dynamics. Here, we investigate chain dynamics of PEO as a function of salt concentration. The self-diffusion coefficient of species i is given as[26]

$$D_i = \lim_{t\to\infty} \frac{\langle \mathbf{R}^2{}_i(t) \rangle}{6t} \tag{7}$$

where $\mathbf{R}_i(t)$ is the displacement of the center-of-mass of species i during time t. Here, the species can be either an ion, a complex, or a polymer chain. The brackets indicate an ensemble average. For polymers, it is also instructive to monitor the end-to-end vector autocorrelation function given as

$$P_1(t) = \langle \mathbf{e}(t) \cdot \mathbf{e}(0) \rangle \tag{8}$$

where $\mathbf{e}(t)$ is a unit vector lying along the end-to-end vector for a given chain. For unentangled polymer chains, the Rouse model yields[27]

$$P_1(t) = \sum_{p=1,3,5\ldots} \frac{8}{p^2\pi^2} \exp[-tp^2/\tau_R] \tag{9}$$

where τ_R is the Rouse time, or longest relaxation time, of the chains. The center-of-mass diffusion coefficients and Rouse times (from fitting eq 9 to the end-to-end vector ACF) for PEO as a function of composition and temperature are shown in Table 4. The end-to-end vector ACF are well described by eq 9, indicating that application of the Rouse model to the unentangled PEO/salt solutions is reasonable.

As we expected, the self-diffusion coefficient of PEO decreases with increasing salt content and decreasing temperature. Comparing with Table 1, the influence of salt on the polymer self-diffusion coefficient is much greater than on the conformational transition time. Similarly, the Rouse time increases dramatically with increasing salt concentration. Unlike the case for conformational transitions, the influence salt on both the self-diffusion coefficient and Rouse time is much greater at the lower temperature. Conversely, it is apparent that the effect of decreasing temperature on the chain dynamics increases dramatically with increasing salt concentration. This behavior is consistent with the experimentally observed increase in the polymer glass transition temperature with increasing salt concentration.[20,21]

It is also possible, for some of the simulated systems, to look at the dynamics of complexed and uncomplexed chains individually. A chain is considered to be com-

Table 4. Polymer Mobilities

	overall				complexed		uncomplexed	
	D (10^{-7} cm^2/s)		τ_R (ns)		D (10^{-7} cm^2/s)		D (10^{-7} cm^2/s)	
system	450 K	363 K	450 K	363 K	450 K	363 K	450 K	363 K
pure PEO	31	8.4	0.5	2.2	n/a[a]	n/a	n/a	n/a
48:1	19	4.9	0.7	5.4	9.5	1.0	21	5.1
15:1	10	0.7	1.0	11.5	7.9	0.5	13	1.2
15:1 X-linked[b]	2.0	n/s[c]	n/a	n/s	n/a	n/s	n/a	n/s
5:1	0.3	0.045	33	250	*d*			

[a] Not applicable. [b] Cross-linked system, see text. [c] Not simulated. [d] Not calculable.

plexed when four or more of its oxygen atoms are complexed with Li^+ cations. The self-diffusion for complexed and uncomplexed chains (chains with three or fewer oxygen atoms complexing Li^+ cations) are given in Table 4 for the 48:1 and 15:1 systems at 450 and 363 K. For both temperatures the self-diffusion coefficient of the complexed chains shows only a weak dependence on salt concentration. This is consistent with the division of the dilute (EO:Li ≥ 15:1) solutions into salt-rich domains and pure polymer-like domains discussed in our previous paper.[11] Complexed chains reside in salt-rich domains whose structure and, apparently, conformational (see above) and chain dynamics are nearly independent of composition in the dilute regime. The self-diffusion coefficient of the uncomplexed chains shows a strong composition dependence in the dilute regime, despite the fact that the conformational dynamics of these chains closely resemble those of pure PEO. For EO:Li = 15:1, the uncomplexed chains are much more likely to interact with the dynamically slower salt-rich domains, subsequently slowing their center-of-mass displacement relative to uncomplexed chains at EO:Li = 48:1 without perturbing their conformational dynamics.

IV. Lifetime of Ether Oxygen−Li^+ Cation and I^-−Li^+ Bonds

It was shown in our previous work[11] that a Li^+ cation is solvated in the PEO host by means of a PEO segment (commonly containing six ether oxygen atoms) wrapping around the cation. The coordinating oxygen atoms tend to exclude I^- anions from the Li^+ coordination shell; the stronger the Li^+/PEO segment interaction, the lower the probability of I^- anions participating in the solvation of the cation and hence the greater the probability of free cation formation. But strong Li^+/PEO segment interactions may also restrict Li^+ cation motion. For example, nonlabile cation/polymer bonding results in essentially zero cation conductivity for systems above the entanglement molecular weight.[6]

The lifetime of the EO−Li^+ cation bond is a good indicator of the lability of the Li^+/PEO segment interactions. An EO−Li^+ bond is considered to exist as long as the ether oxygen remains continuously within the first coordination shell (4.0 Å) of the cation. Only those ether oxygen atoms, however, that reached the position of the first peak of the Li−O radial distribution function (2.1 Å) inside the Li^+ cation coordination shell were considered to form a stable EO−Li^+ bond and therefore were included in the statistics. The probability of a Li^+−EO bond having lifetime longer than τ_{Li^+-EO} is shown in Figure 5 at 450 K. Probabilities of Li^+−EO bond lifetimes are similar for all compositions, with a slight increase in the probability of long-lived Li^+−EO bonds at high salt concentration. The majority of Li^+−EO bonds last less than 100 ps, indicating that the bonds

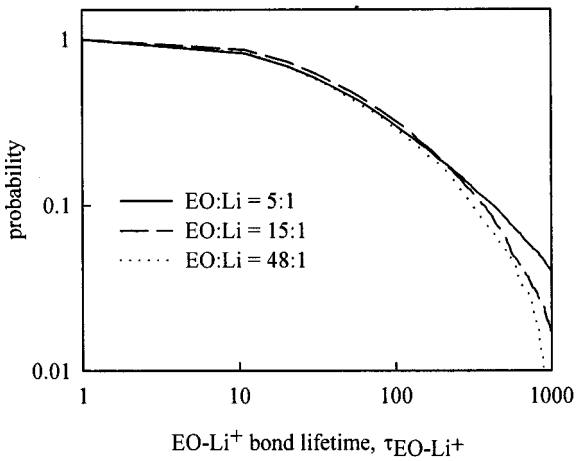

Figure 5. Probability of Li^+−EO bond lifetime at 450 K.

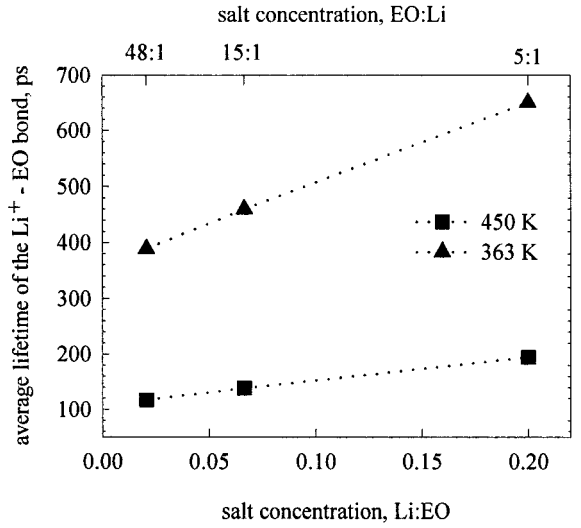

Figure 6. Average lifetime of the Li^+−EO bond as a function of salt concentration at 363 and 450 K.

are quite labile. The average bond lifetime of the Li^+−EO bond is shown in Figure 6. The lifetime of the Li^+−EO bond increases with increasing salt concentration and decreasing temperature, thus correlating with the slowing down of conformational dynamics at high salt concentrations and low temperatures.

The average lifetime of the I^-−Li^+ (τ_{I-Li}) bond was calculated analogously to the lifetime of the Li^+−EO bond τ_{Li^+-EO}. At 450 K and low salt concentration (EO:Li = 48:1 and EO:Li = 15:1) τ_{I-Li} was found be of the order of 700−800 ps, and at high salt concentration (EO:Li = 5:1) τ_{I-Li} = 500 ps. The drop in the average lifetime of the I^-−Li^+ bond at high salt concentration is connected to the increased competition of I^- anions for Li^+ due to the formation of larger ionic aggregates.

Table 5. Ion Mobilities, Conductivity, and Transfer Number

	D (10^{-7} cm^2/s)						σ (10^{-4} S/cm)		t_+[a]	
	Li^+		I^-		collective					
system	450 K	363 K	450 K	363 K	450 K	363 K	450 K	363 K	450 K	363 K
pure PEO										
48:1	11.0	2.6	11.5	2.8	0.30	0.27	0.7	0.8		
15:1	6.4	0.61	6.7	0.71	0.34	0.23	2.2	2.0	~0.1	~0.1
15:1 (cross-linked)	3.0		3.2		0.25		1.6		~0.1	
EO:Li = 5:1	0.30	0.045	0.29	0.045	0.03	0.002	0.5	0.05	~0.5	~0.5

[a] Transfer number, see eq 12.

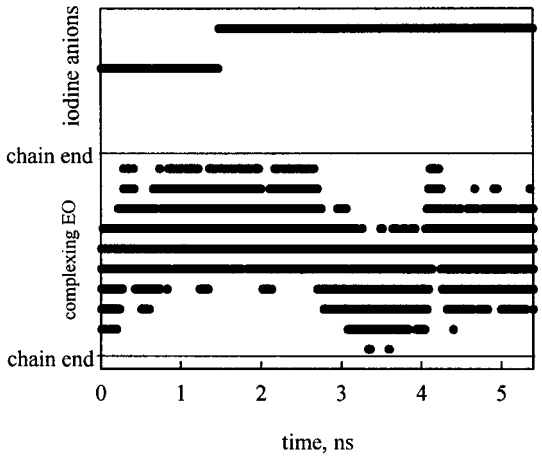

Figure 7. Ether oxygen atoms and I^- anions in the first coordination sphere (4.0 Å) of a Li^+ cation. Results for a 5.6 ns trajectory of EO:Li = 15:1 system at 450 K are presented. The abscissa shows the relative position (index) of the 10 EO atoms involved in complexation, all of which belong to the same PEO chain. The I^- index is arbitrary.

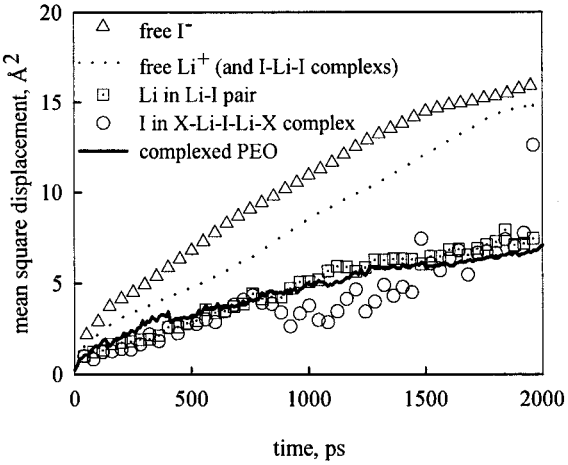

Figure 8. Mean-square displacements of ions, ion aggregates, and complexed PEO as a function of time. Results are shown for the EO:Li = 15:1 system at 363 K. X denotes the possibility of having one or more ions belonging to a given aggregate.

V. Ion Mobility and Conductivity

Ion Mobility and Correlation with Polymer Motion. Ion self-diffusion coefficients (defined by eq 7) are important indicators of ion mobility. The cation and anion self-diffusion coefficients are given in Table 5. The self-diffusion coefficient for Li^+ at 363 K for the 15:1 system is of the same order of magnitude as that obtained from PFG NMR measurements of a PEO/$LiCF_3SO_3$ system at the same temperature,[6,28] indicating reasonable agreement between simulation and experiment.

The strong correlation between ion self-diffusion and polymer self-diffusion is clearly demonstrated when the self-diffusion coefficients of the ions are compared with those of the polymer in Table 4. The ion self-diffusion coefficients are somewhat lower than those of polymer for EO:Li ≥ 15:1 solutions, perhaps due to the high mobility of uncomplexed chains. For the EO:Li = 5:1 solutions, all chains are complexed, and the ion mobility appears to be equal to or even greater than that of the polymer. It should be kept in mind that the uncertainties in results reported for the EO:Li = 5:1 solutions at 363 K are relatively large, as the Rouse time is considerably longer than the simulation trajectory.

The correlation between polymer center-of-mass motion and ion motion indicates that despite the highly labile nature of the cation/polymer bond, as discussed above, the cation has a strong tendency to move with a particular polymer chain. This is demonstrated in Figure 7. Here, it can be seen that, during the 5.6 ns duration of the simulation, a particular cation moves from one end of a PEO chain to the other several times but does not jump from one chain to another. After about 1.5 ns, the I^- anion involved in complexing Li^+ cation diffuses away and is replaced by the other anion.

Mobility of Ionic Aggregates. The binding of the anion to the polymer is significantly weaker than that of the cation.[13] Hence, on first glance it is surprising that the anion motion is apparently as strongly correlated with the polymer motion as that of the cation. However, the self-diffusion coefficients given in Table 5 consider all anions, most of which are bound to cations in pairs and larger complexes. It is therefore instructive to look at the mobilities of free ions, ion pairs, and other complexes individually. The charged complexes contribute to the overall ionic conductivity, while the neutral complexes (e.g., pairs) do not (see below). We define Li^+ cations and I^- anions as free when they do not have any other ions within 4.0 Å.[29] A Li−I ion pair is considered to form if the cation and anion are within 4.0 Å of each other and no other ions are within 4.0 Å from either of them. $Li^+-(\mathbf{I}^-)-Li^+$ and $I^-(\mathbf{Li}^+)-I^-$ and higher aggregates are defined analogously. The PEO/LiI system at 363 K and salt concentration of EO:Li = 15:1 has a sufficient number of free ions, ion pairs, and aggregates in order to individually monitor their mean-square displacements, which are shown in Figure 8. Qualitatively similar results were obtained for the other simulated temperatures and concentrations, but the paucity of free ions at 450 K and the small number of ions for the EO:Li = 48:1 solutions precluded us from analyzing temperature and concentration behavior of the diffusion of each species.

Somewhat unexpectedly, free Li^+ cations and $I^-(Li^+)-I^-$ aggregates have approximately the same mobility and hence are shown as a combined curve in Figure 8. Free I^- anions have the highest mobility as a consequence of their weak interaction with the polymer

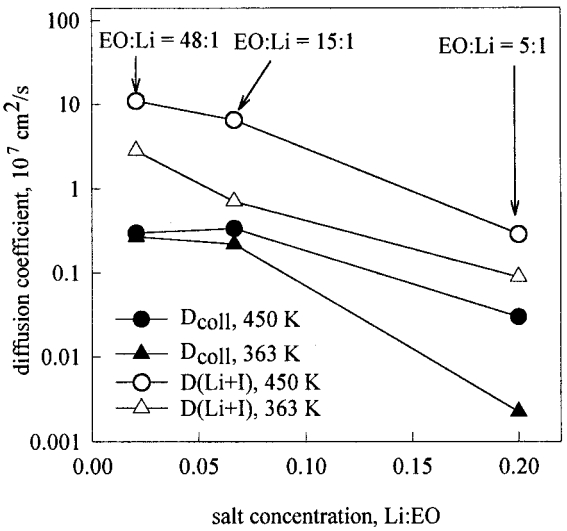

Figure 9. Collective ion diffusion coefficients (D_{coll}) and average ion diffusion coefficients as a function of salt concentration at 363 and 450 K. The average ion diffusion coefficient is the mean of the Li^+ and I^- self-diffusion coefficients.

host. The mobilities of Li−I pairs, and aggregates involving two or more Li atoms, were the lowest. Hence, we find $D_{I^-} > D_{Li^+} \cong D_{I^-(Li^+)-I} > D_{LiI} \geq D_{\text{aggregates of two-Li and more}}$. The near equal mobility of Li^+ cation and $I^-(Li^+)I^-$ aggregates (note that the latter cluster is much larger) is due to a much weaker $I^-(Li^+)I^-$—PEO interaction than for free Li^+—PEO interactions, resulting in a partial decoupling of $I^-(Li^+)I^-$ motion from the polymer motion. In fact, Li^+ cations in $I^-(Li^+)I^-$ clusters tend to be coordinated by only three ether oxygen atoms, while free Li^+ cations are most probably coordinated by six contiguous ether oxygen atoms. Decoupling of ion motion from polymer motion is further discussed in section VI.

Collective Motion and Conductivity. The self-diffusion coefficients of the ions do not yield the conductivity of the system, as they do not reflect correlated motions of cations and anions. For example, a cation−anion pair moving together would contribute to the self-diffusion coefficients of both species but would contribute nothing to the charge flux or conductivity. To monitor net charge transport, we calculated a collective ion diffusion coefficient D_{coll}, which reflects net ion transfer[26]

$$D_{coll} = \lim_{t\to\infty} \frac{1}{N_{Li} + N_I} \sum_{i=1}^{N_{Li}} \sum_{j=1}^{N_I} z_i z_j \mathbf{R}_i(t)\cdot\mathbf{R}_j(t) \qquad (10)$$

Here, i and j refer to cations and anions, respectively, and z is the charge of the ion in the electron charge units, and N_{Li}, N_I are the number of Li^+ cations and I^- anions in the system. The conductivity of the system is given by the relation[26]

$$\lambda = \frac{e^2(N_{Li} + N_I)}{Vk_BT} D_{coll} \qquad (11)$$

where V is the volume of the simulation cell, T is temperature, t is time, and e is an electron charge. The collective diffusion coefficients and conductivities for the various systems are given in Table 5. The large difference between uncorrelated and collective ion self-diffusion coefficients shown in Figure 9 indicates that cation and anion motions are highly correlated. The ion self-diffusion coefficient shows almost exponential decrease with increasing salt concentration, while the collective ion diffusion coefficient does not exhibit significant changes upon salt concentration increase from EO:Li = 48:1 to EO:Li = 15:1, while on further addition of salt it drops dramatically.

Conductivity. Conductivities determined from eq 11 are given in Table 5. We were unable to find experimental studies of the conductivity of PEO/LiI solution for low molecular weight at high temperatures (above the PEO melting point) for the concentration range explored in our simulations. Experimental data are available, however, for high molecular weight PEO/LiI systems. It is instructive to compare our conductivity values for our low molecular weight PEO/LiI system at 363 K with the experimental values for high molecular weigh (5×10^6 Da) PEO/LiI system at 357 K.[30] For EO:Li = 25:1 a value of 3×10^{-4} S/cm and for EO:Li = 11:1 a value 1×10^{-4} S/cm were obtained. In another experimental study[31] at EO:Li = 4.5:1 at 363 K for LiI salt/high molecular weight PEO a conductivity of 1.5×10^{-5} S/cm was obtained. These results are in satisfactory agreement with the conductivity values obtained from our simulations. Taking into account that conductivity usually increases with decreasing molecular weight,[6,22,32] conductivity from our simulations appears to be about an order of magnitude lower than experiment after molecular weight correction. In addition, Table 5 indicates a maximum in conductivity as a function of composition occurring around EO:Li ≈ 15:1, consistent with experiment.[30]

Li^+ Transfer Number. It is important to understand which ionic species (Li^+ or I^-) dominate in the charge-transfer process. We define the Li^+ transfer number t_+ in the following way

$$t_+ = 0.5 + \frac{D_{Li^+} - D_{I^-}}{D_{coll}} \qquad (12)$$

where D_{Li^+} and D_{I^-} are the self-diffusion coefficients of Li^+ cation and I^- anion, respectively, and D_{coll} is the collective ion diffusion coefficient defined above. At the lowest salt concentration (EO:Li = 48:1) accurate determination of the ion self-diffusion coefficient is precluded by the small number of ions in the system and therefore poor statistics, while at the highest salt concentration ions move very slowly, which decreases absolute values and therefore increases relative error in the determination of self-diffusion coefficients. For both cases, the uncertainty in $(D_{Li^+} - D_{I^-})/D_{coll}$ is large. Therefore, we consider the Li^+ transfer number (shown in Table 5) only qualitatively. At low salt concentration charge transfer is dominated by the anion, while at high salt concentration (EO:Li = 5:1) charge is approximately equally transferred by cations and anions. In experimental measurements of the Li^+ transfer number in a high molecular weight PEO/LiI solution at 343 K, the Li^+ charge transfer number was found to drop quickly with decreasing salt concentration, exhibiting a minimum value of about 0.15 between 10 and 20 mol % of LiI.[30] These results are in a qualitative agreement with our simulations.

VI. Discussion

Our simulations reveal a dramatic influence of salt on polymer dynamics and an intimate relationship

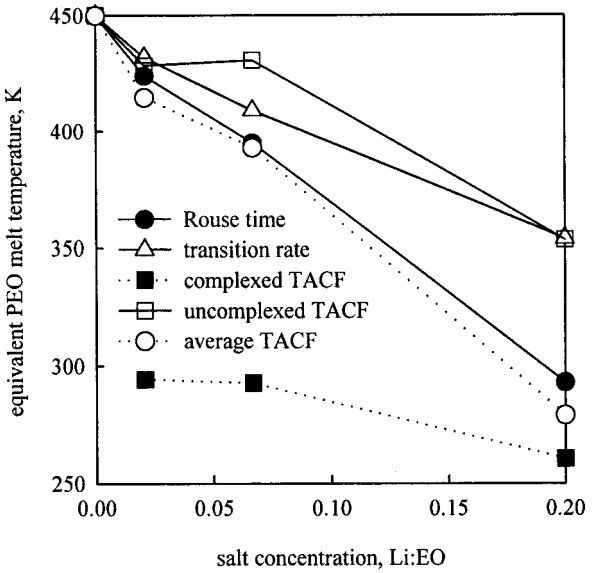

Figure 10. Equivalent PEO melt temperatures for various dynamic properties of the PEO/LiI solutions as a function of salt concentration at 450 K. Transition rates and torsional correlation times are for the C—O bond.

between polymer and ion motions. Here, we summarize our results and discuss possible mechanisms for these effects.

A. Influence of Salt on Polymer Dynamics. We observed a reduction in both conformational and chain dynamics for the polymer with increasing salt concentration. Salt has a relatively small influence on the rate of conformational transitions but a dramatic influence on the torsional autocorrelation function. At lower salt concentrations (EO:Li ≥ 15:1), the reduction in the rate of conformational dynamics is mainly due to complexation of PEO dihedrals with Li^+ cations. At high concentration (EO:Li = 5:1), both complexation and increased conformational cooperativity play a role in slowing conformational dynamics. Chain dynamics (self-diffusion coefficient and the Rouse time) are also dramatically influenced by salt. Possible mechanisms for the slowing of polymer chain dynamics include the reduction in the rate of conformational transitions observed for complexed dihedrals, restriction of conformational space available to complexed dihedrals, and the formation of transient cross-links between chains. Similar effects on polymer dynamics observed with increasing salt concentration are seen in pure polymer melts with decreasing temperature.[16,25,33] Because of the apparent similarity in the effect of temperature and salt on polymer dynamics, we have explored the concept of temperature/concentration correspondence in order to gain insight into the influence of salt on polymer dynamics.

The rate of conformational transitions in pure PEO melts exhibits Arrhenius behavior over a wide temperature range, while the Rouse time exhibits Vogel—Fulcher behavior.[16,33] Exploiting these characteristics, we have determined the temperature at which pure PEO has the same rate of conformational transitions and the temperature at which pure PEO has the same Rouse time as the PEO/LiI solutions at 450 K as a function of composition. These results are shown in Figure 10. Similar behavior is seen at 363 K. The figure clearly demonstrates that the influence of salt is much greater on chain dynamics (Rouse time) than on the rate of conformational transitions, particularly at high salt concentration. Therefore, we cannot attribute the increase in Rouse time with increasing salt concentration exclusively, or even largely, to a reduction in the rate of conformational transitions. This is consistent with simulations of pure melts near the glass transition temperature.[16,33]

In simulations of pure PEO melts, it was seen that the temperature dependence of the torsional correlation time (time integral of the TACF) and that of the Rouse time showed similar Vogel—Fulcher behavior.[16,33] This would lead us to anticipate much closer temperature/concentration correspondence for the TACF and the Rouse time than was observed for the conformational transition rate and the Rouse time. However, the dynamic heterogeneity introduced in the system by having both complexed and uncomplexed dihedrals significantly increases the torsional correlation time, precluding us from elucidating meaningful temperature/concentration correspondence for the torsional correlation time for the overall TACF. To avoid this problem, we can investigate the behavior of the TACF for the complexed and uncomplexed dihedrals individually and determine an average equivalent PEO temperature by weighting the equivalent temperatures for the complexed and uncomplexed torsional correlation times by their respective fraction (Table 2). The torsional correlation times were estimated from the KWW fits to the TACF for the complexed and uncomplexed dihedrals (Table 2).

The temperature/concentration correspondence seen in Figure 10 indicates that the decrease in the rate of chain dynamics with increasing salt concentration is strongly correlated with an increase in the torsional correlation time. Similar behavior is seen in pure PEO melts,[33] where conformational space available to a dihedral is restricted on increasingly longer time scales with decreasing temperature. This restriction is a consequence of the increasingly cooperative nature of transitions required for a given dihedral to visit all conformations as the system vitrifies.[25,33] For the polymer/salt solutions, restriction of conformational space can be associated with the limited number of polymer conformations that can effectively complex a Li^+ cation.[11] This restriction becomes more extreme at high salt concentration due to the involvement of most neighboring dihedrals in cation complexation.

The above picture of temperature/concentration correspondence does not invoke transient cross-links to account for the influence of salt on polymer chain dynamics. However, transient cross-links are quite common in our systems. These cross-links consist either of a Li^+ cation being complexed by oxygen atoms from two chains, or of $Li^+—I^-—Li^+$ complexes, which predominately involve two chains. At 450 K, approximately half of the I^- anions are involved in transient cross-links, while direct Li^+ cross-links are rare. At 363 K, the increase in the number of free ions results in an increase in direct Li^+ cross-links and a decrease in $Li^+—I^-—Li^+$ complexes. Consequently, the total number of cross-links/ion is not dramatically dependent upon the composition or temperature.

The influence of these cross-links on chain dynamics is difficult to quantify. The lifetime of $Li^+—I^-$ bonds is around 400—600 ps at 363 K and 100—150 ps at 450 K (see section IV). These times are much shorter than the Rouse times for the PEO chains, even for the lowest salt

concentration. The lifetime of the direct Li^+ cross-link depends strongly upon concentration—it is on the order of a nanosecond for EO:Li = 15:1 and 50 ps for EO:Li = 5:1. The short lifetime at high salt concentration is due to increased competition of the Li^+ cations for ether oxygen atoms. The lifetime of the direct Li^+ cross-links is much shorter than the Rouse time at higher salt concentration and lower temperature. We therefore believe that while it is likely that transient cross-links do influence chain dynamics, they are not the dominant in determining the influence of salt on the polymer.

B. Mechanisms of Ion Motion. The strong coupling of the polymer center-of-mass and ion motions for our low molecular weight PEO chains is discussed above. It has been observed experimentally that while the mobility of Li^+ in PEO decreases with increasing molecular weight,[6] the effect saturates at a molecular weight corresponding to approximately the entanglement molecular weight. This has been interpreted in terms of a change in mechanism from diffusion of the cation with the polymer chain for low molecular weight to a mechanism dominated by interchain (or intersegment) hopping when the polymer center-of-mass motion becomes sufficiently slow, the so-called dynamic bond percolation theory.[7] Here, we examine our simulations in order to determine whether our results are consistent with these mechanisms.

1. Transient Cross-Links and Interchain Hopping. It has been widely accepted[1,2] that the Li^+ cation can be complexed by two PEO chains (or two different segments of a long PEO chain), thus serving as a transient cross-linking center between these two chains. As mentioned above, such direct Li^+ transient cross-links have been observed in our simulations. The formation of such a cross-link is a necessary but not sufficient condition for a cation to transfer from one chain to another, i.e., for an interchain hop to occur. We found interchain hopping events to be rare. In our simulations, cation interchain transfer was observed only among a fraction of direct Li^+ transient cross-links with a lifetime longer than 500 ps. On the basis of the required lifetime of the transient cross-link, the rarity of such long-lived cross-links, and the fraction of such cross-links that result in an interchain hop, we estimate a frequency of 1 interchain hop/cation/10−100 ns. Conversely, we can consider each Li^+ cation as undergoing an interchain hop every 10−100 ns.

2. Decoupling of Polymer/Ion Motion. Referring to Tables 4 and 5, we can see that the self-diffusion coefficient for Li^+ and I^- are around 50%−60% of that of the polymer center-of-mass for EO:Li ≥ 15:1 at both 450 and 363 K. As mentioned above, the larger self-diffusion coefficient for uncomplexed chains may account for the fact that the self-diffusion coefficient of the polymer is somewhat larger than that of the ions. In any event, for these concentrations, where the estimated interchain hopping time is greater than the Rouse time, the ion mobility and polymer mobility are strongly coupled. For the EO:Li = 5:1 system, τ_R is comparable to (450 K) or longer than (363 K) the estimated interchain hopping time. For these solutions, the ion self-diffusion coefficient is equal to (450 K) or even greater than (363 K) that of the polymer, indicating a partial decoupling of the polymer and ion motions.

A thorough investigation of the influence of molecular weight on ion mobility is of great interest but is beyond the computational scope of this work. However, to investigate possible decoupling of ion and polymer motions at higher molecular weight, we performed limited simulations on our EO:Li = 15:1 system with two random cross-links per chain. Such a system resembles a highly branched PEO chain having 384 repeat units. The PEO self-diffusion coefficient, as well as the cation and anion diffusion coefficients and conductivity for this system at 450 K, are given in Tables 4 and 5, respectively. The "apparent" self-diffusion coefficient of the polymer decreased by a factor of 5,[34] while those for the ions decreased by a factor of 2, upon cross-linking. The conductivity decreased only by 30% despite the severe slowing of polymer motion. Hence, increasing molecular weight leads to a partial decoupling of the motion of the ions from that of the polymer chain similar to that seen with increasing salt concentration.

For a 20:1 PEO/$LiCF_3SO_3$ system at 363 K,[6] ion diffusion is observed experimentally to be independent of molecular weight for $M_W \geq 3200$ Da (the entanglement molecular weight) and to increase with decreasing molecular weight for $M_W < 3200$ Da. Assuming the applicability of the dynamic bond percolation theory, and that the Rouse model provides a good description of unentangled polymer dynamics in the polymer/salt solutions, the time scale for interchain hopping must be smaller than τ_R for the 3200 Da system. We can estimate the Rouse time for our EO:Li = 15:1 PEO/LiI solution at 3200 Da and 363 K as $\tau_R = (3200/540)^2 \times 11.5$ ns = 400 ns. This time should be similar to the Rouse time for the 20:1 PEO/$LiCF_3SO_3$ system at the same temperature and molecular weight. The Rouse time is longer (400 ns) than the estimated interchain hopping time (10−100 ns); this supports the dynamic bond percolation mechanism for ion diffusion in high molecular weight PEO and indicates that our simulation based estimate for the interchain hopping time is reasonable.

Acknowledgment. The authors are indebted to the National Science Foundation—Division of Materials Research for support through NSF CARRER award DMR 96-24475 and to the Eveready Battery Company for a gift which allowed continuation of this project. An allocation of computer time from the center for the High Performance Computing at the University of Utah is gratefully acknowledged. We also thank R. L. Jaffe, R. Boyd, and D. Bedrov for helpful discussions.

References and Notes

(1) Gray, F. M. *Polymer Electrolytes*; The Royal Society of Chemistry: Cambridge, 1997.
(2) Bruce, P. G.; Vincent, C. A. *J. Chem. Soc., Faraday Trans* **1993**, *89*, 3187.
(3) Abraham, K. M.; Jiang, Z.; Carroll, B. *Chem. Mater.* **1997**, *9*, 1978.
(4) Tsuchiya, J. *Mater. Res. Soc. Symp. Proc.* **1998**, *135*, 357.
(5) Reiche, A.; Tûbker, J.; Siury, K.; Sander, B.; Fleischer, G.; Waterwing, S.; Shashkov, S. *Solid Sate Ionics* **1996**, *85*, 121.
(6) Shi, J.; Vincent, C. A. *Solid State Ionics* **1993**, *60*, 11.
(7) Ratner, M. A. *Polymer Electrolyte Review−1*; Elsevier: Amsterdam, 1989; Chapter 7.
(8) Muller-Plather, F.; van Gunsteren W. F. *J. Chem. Phys.* **1995**, *103*, 4745.
(9) Muller-Plather, F. *Acta Polym.* **1994**, *45*, 259.
(10) Neyertz, S.; Brown, D. *J. Chem. Phys.* **1996**, *104*, 3797.
(11) Borodin, O.; Smith, G. D. *Macromolecules* **1998**, *31*, 8396.
(12) Smith, G. D.; Jaffe, R. L.; Yoon, D. Y. *J. Phys. Chem.* **1993**, *97*, 12752.
(13) Smith, G. D.; Jaffe, R. L.; Partridge, H. *J. Phys. Chem. A* **1997**, *101*, 1705.

(14) Londono, J. D.; Annis, B. K.; Habenschuss, A.; Borodin, O.; Smith, G. D.; Turner, J. Z.; Soper, A. K. *Macromolecules* **1997**, *30*, 7151.
(15) Smith, G. D.; Yoon, D. Y.; Jaffe, R. L.; Colby, R. H.; Krishnamoorti, R.; Fetters, L. J. *Macromolecules* **1996**, *29*, 3462.
(16) Smith, G. D.; Yoon, D. Y.; Wade, C. G.; O'Leary, D.; Chen, A.; Jaffe, R. L. *J. Chem. Phys.* **1997**, *106*, 3798.
(17) Berthier, C.; Gerecki, W.; Minier, M.; Armand, M. B.; Chabango, J. M.; Rigaud, P. *Solid State Ionics* **1983**, *11*, 91.
(18) Jaffe, R. L.; Smith, G. D.; Yoon, D. Y. *J. Phys. Chem.* **1993**, *97*, 12745.
(19) Ryckaert, J. P.; Ciccotti, G.; Berendsen, H. J. C. *J. Comput. Phys.* **1977**, *23*, 327.
(20) Torell, L. M.; Angel, C. A. *Br. Polym. J.* **1988**, *20*, 173.
(21) Killis, A.; Le Nest, J.-F.; Gandini, A.; Cheradame, H. *Macromolecules* **1984**, *17*, 63.
(22) Gray, F. M. *Solid State Ionics* **1990**, *40*−*41*, 637.
(23) Vachon, C.; Vasco, M.; Perrier, M.; Prud'homme, J. *Macromolecules* **1993**, *26*, 4023.
(24) Vachon, C.; Labreche, C.; Vallee, A.; Besner, S.; Dumont, M.; Prud'homme, J. *Macromolecules* **1995**, *28*, 5585.
(25) Boyd, R. H.; Gee. R. H.; Han, J.; Jin, Y. *J. Chem. Phys.* **1994**, *101*, 788.
(26) Toda, M.; Kubo, R.; Saito, N. *Statistical Physics I, Equlibrium Statistical Mechanics*, 2nd ed.; Springer: Heidelberg, Germany, 1995.
(27) Doi, M.; Edwards, S. F. *The Theory of Polymer Dynamics*; Clarendon Press: Oxford, 1992.
(28) The experimental data were interpolated to a $M_W = 540$ Da.
(29) Solvent-separated ion pairs[1,2] were considered as free ions. Longer simulation time scales and bigger size of the simulation box are required in order to unambiguously determine diffusion coefficients for solvent-separated ion pairs.
(30) Lobitz, P.; Fullbier, H.; Illner, J. C.; Reuter, H.; Horing, S. *Solid State Ionics* **1992**, *58*, 41.
(31) Chabagno, J. M. Thesis, University of Grenoble, Grenoble, France, 1980.
(32) Lobitz, A.; Fullbier, H.; Rieche, A.; Ambrahsat, K. *Solid State Ionics* **1992**, *58*, 49.
(33) Borodin, O.; Bedrov, D.; Smith, G. D. Manuscript in preparation.
(34) The self-diffusion coefficient of the polymer continues to decrease with increasing length of simulation. The ion self-diffusion coefficients appear to have stabilized.

MA991429H